Techno-economic Analysis of Contingency Reserve Allocation Scheme for Combined UHV DC and AC Receiving-End Power System

Di Wu, *Student Member, IEEE*, Ning Zhang, *Member, IEEE*, Chongqing Kang, *Senior Member, CSEE, Senior Member, IEEE*, Yi Ge, Zhenjian Xie, and Junhui Huang

***Abstract*—In a UHV DC and AC combined system the UHVDC's blocking fault becomes the most serious load balance contingency of the receiving end power system due to its large capacity. The amount of contingency reserve thus is largely increased. This paper proposes three distinct schemes for allocating contingency reserve to cover the power shortage caused by UHVDC's blocking fault, and compares the economic cost of these schemes. An operation simulation method using a unit commitment technique is proposed for evaluating the operation costs associated with increasing contingency reserve. A real case study for a Jiangsu Province power system in China is presented to demonstrate that the best scheme is to share the contingency reserve with neighborhood power systems through the transmission capacity of UHVAC lines.**

***Index Terms*—Contingency reserve, operation cost, operation simulation, UHV DC and AC combined system, UHVDC blocking fault.**

NOMENCLATURE

A. Indices and Numbers

N	Number of UHVAC channels of the receiving end of UHV DC and AC combined system linking with other areas.
m	Number of UHVAC transformers in the receiving end of UHV DC and AC combined system.
n	Investment recovery period, which is usually 25 years.
f, c, w, s, h	Subscripts denoting generating units: those that start and stop daily, cannot start and stop daily, wind farms, solar units, and regular or pumped hydro units.
T	Superscript denoting transposition.

B. Continuous Variables

C_1, C_2, C_3	Extra annual cost of contingency reserve for UHVDC brings to the power system for the three contingency reserve allocation schemes provided in the paper.
C_{op}^0	Original annual operation cost of the power system that does not consider the contingency reserve for UHVDC blocking fault.
C_{op}	Operation cost that considers the contingency reserve for UHVDC.
C_{ls}	Annual cost caused by load shedding.
C_{in}	Annual value of investment cost of UHVAC proportional to the spare capacity needed.
VOLL	Cost value of unit load loss.
EENS	Expected energy not supplied caused by the UHVDC blocking fault.
P_{DC}	Largest capacity of UHVDC projects of the receiving end of UHV DC and AC combined system.
P_{AC}	Average capacity of UHVAC projects of the receiving end of UHV DC and AC combined system.
$I_{\text{line,annual}}$	Annual cost of UHVAC lines.
$I_{\text{trans,annual}}$	Annual cost of UHVAC transformers.
I_{line}	Investment cost of per unit length UHVAC line.
I_{trans}	Investment cost of UHVAC transformers that transfer the energy from 1000 kV Power grid to the 500 kV power grid.
l	Length of the UHVAC line linked the target area with other areas.
R_{con}	Contingency reserve scheduled for the UHVDC blocking fault in the receiving end of UHV DC and AC combined system.
$\boldsymbol{D}^t$	Column vector of nodal loads at t.
$\boldsymbol{D}_{\text{d}}^t$	Column vector of nodal load shedding at t.
$\boldsymbol{C}_{\text{f}}, \boldsymbol{C}_{\text{c}}, \boldsymbol{C}_{\text{w}}, \boldsymbol{C}_{\text{s}}$	Column vector of average cost of different types of generation.
$\boldsymbol{C}_{\text{d}}$	Column vector of load shedding cost.
$\boldsymbol{C}_{\text{wd}}$	Column vector of wind curtailment cost.
$\boldsymbol{C}_{\text{sd}}$	Column vector of solar curtailment cost.
$\boldsymbol{V}_{\text{f}}$	Column vector of start-stop cost of generating units that can start and stop daily.

Manuscript received January 2, 2016; revised March 18, 2016; accepted April 13, 2016. Date of publication June 30, 2016; date of current version May 18, 2016. This work was jointly supported by National Natural Science Foundation of China (No. 51325702), Science-Technology Project of State Grid Corporation of China (No. GHJS1500009), and State Grid Excellent Innovation Foundation of Tsinghua University (No. 2011079).

D. Wu, N. Zhang, and C. Kang (corresponding author, e-mail: cqkang@tsinghua.edu.cn) are with State Key Laboratory of Power Systems, Department of Electrical Engineering, Tsinghua University, Beijing 100084, China.

Y. Ge, Z. Xie, and J. Huang are with the Economic Research Institute of Jiangsu Electric Power Company, Nanjing 210008, China.

DOI: 10.17775/CSEEJPES.2016.00023

$\boldsymbol{S}_{\mathrm{f}}^{t}$ Column vector of start-stop cost of generating units that can start and stop daily at t.

$\boldsymbol{P}_{\mathrm{f}}^{t}, \boldsymbol{P}_{\mathrm{c}}^{t}, \boldsymbol{P}_{\mathrm{w}}^{t}, \boldsymbol{P}_{\mathrm{s}}^{t}, \boldsymbol{P}_{\mathrm{h}}^{t}$ Column vector of output of different types generation at t.

$\boldsymbol{D}_{\mathrm{h}}^{t}$ Column vector of dispatched pumping load of hydro units at t (not applicable to regular hydro units).

$\boldsymbol{P}_{\mathrm{wf}}^{t}$ Column vector of forecast wind power at t.

$\boldsymbol{P}_{\mathrm{wd}}^{t}$ Column vector of wind power curtailed at t.

$\boldsymbol{P}_{\mathrm{f\,max}}, \boldsymbol{P}_{\mathrm{f\,min}}, \boldsymbol{P}_{\mathrm{c\,max}}, \boldsymbol{P}_{\mathrm{c\,min}}, \boldsymbol{P}_{\mathrm{w\,max}}, \boldsymbol{P}_{\mathrm{s\,max}}, \boldsymbol{P}_{\mathrm{h\,max}}, \boldsymbol{P}_{\mathrm{h\,min}}$ Column vector of maximum and minimum power of different types of generation.

$\Delta\boldsymbol{P}_{\mathrm{fdown}}, \Delta\boldsymbol{P}_{\mathrm{fup}}, \Delta\boldsymbol{P}_{\mathrm{cdown}}, \Delta\boldsymbol{P}_{\mathrm{cup}}$ Column vector of maximum and minimum ramping rates of units that start and stop daily and cannot start and stop daily.

$\boldsymbol{G}_{\mathrm{h}}$ Column vector of maximum daily energy generation of regular hydro units or stored energy of pumped hydro units.

C. Binary Variables

$\boldsymbol{I}_{\mathrm{f}}^{t}$ Column vector of the state of units that can start and stop over the dispatching day.

$\boldsymbol{I}_{\mathrm{c}}$ Column vector of the state of units that cannot start and stop over the dispatching day.

D. Constants

r_{reg} Ratio of regulated reserve to the load.

i Discount rate which is usually taken as 0.08.

p_{el} The forced energy loss rate of UHVDC blocking fault.

p_{m} Energy loss percentage caused by monopole trip.

p_{b} Energy loss percentage caused by bipole trip.

η Amplification coefficient of wind curtailment penalty.

δ Amplification coefficient of solar curtailment penalty.

θ Amplification coefficient of load shedding penalty.

γ Amplification coefficient of start-stop cost.

$\boldsymbol{\lambda}$ Column vector of pumping efficiency of pumped storage.

E. Sets

Ω Set of time intervals of daily unit commitment model.

I. Introduction

IN recent years, China's ultra-high-voltage transmission system has been developing rapidly with its power system transitioning from a regionally dominated system to a national UHV DC and AC interconnected power system [1]. The State Grid Corporation of China plans to build the north, central, and east China UHVAC synchronous electric grid, which is expected to have more than 1200 GW generation capacity by 2020. At the same time, there are several UHVDC projects being constructed to realize bulk energy transmission over 2000 km [1].

One of the significant changes that UHVDC brings to the power system is that it would largely increase the contingency reserve requirement. Contingency reserve is the excess capacity required for equipment outages over the forecasted load when committing the generation units [2]. Unlike the regulating reserve that is driven by the uncertainty of load variations, contingency reserve in a power system is usually determined by the largest contingency of single element in terms of capacity. Traditionally, contingency reserve is required to be greater than the capacity of the largest online generator [2]. As the capacity of UHVDC increases, its blocking fault would become the most serious contingency to the receiving end system [3]. The contingency reserve required in the receiving end system should be higher than the UHVDC capacity, which would much larger than before. This kind of contingency reserve would have significant impact to the power system in security and economic aspects [3]. This paper focuses on the economic impact of the increase of contingency reserve for UHVDC injection to the receiving end of UHV DC and AC combined system. It also investigates the most cost-efficient contingency reserve allocation scheme.

In the literature, there are two methods for determining contingency reserve: deterministic and stochastic. The deterministic method adds the constraints of the contingency reserve to the unit commitment model [4], [5]. The contingency method is easy to understand and implement; however, it neglects the power system's stochastic nature, and does not reflect the risk the system faces. Stochastic methods can be further divided into: 1) those that are based on historical statistics that estimate different causes of power imbalance and find the capacity of reserve meeting the reliability target [6]; and 2) those based on stochastic optimization techniques that implicitly blend in the risk index [7] or explicitly consider a range of expected scenarios [8], [9].

In this paper, the deterministic method is used to assess the contingency reserve for two reasons. First, the probability of UHVDC blocking fault is small, which means the stochastic method need not be used. Second, the deterministic method provides a better analysis of the economic impact of the power system.

The method for analyzing contingency reserves in power systems presented in this paper is different from other proposed methods. Studies to date have focused on the energy and reserve joint optimization problem [10], [11], or on the market and pricing problems of reserves when considering renewable energy [12], [13]. However, contingency reserve allocations in UHV DC and AC combined systems have not been considered. In [14] cooperation between the regional grid dispatching system and the provincial dispatching system to handle emergency power support among provinces is considered. In this approach, however, there is no economic analysis at the planning level, and the time scale used is either daily or hourly, and not an entire year's economic analysis for the system.

The main contributions of this paper are as follows: First, three contingency reserve allocation schemes for the receiving end of UHVAC/DC power system are proposed and their economic cost models established. Second, an operation simulation based method is proposed to evaluate the cost of contingency reserve for a whole year's time scale. Third, the optimal contingency reserve allocation scheme is explored for the Jiangsu provincial power system in China.

The rest of this paper is organized as follows. Section II proposes the three contingency reserve allocation schemes and the associated cost calculation method. Section III presents the operation simulation method. Then, Section IV provides the case study of Jiangsu provincial power system. Finally, the conclusion is given in Section V.

II. Three Contingency Reserve Allocation Schemes and Their Associated Costs

A. Contingency Reserve Allocation Schemes

1) Traditional Scheme

In a conventional scheme the capacity of the contingency reserve is chosen as the capacity of the largest unit in the power system so that it can meet the energy imbalance when a largest unit fails. For a large power system, the contingency reserve can also be chosen as a certain fraction of the system load. Currently, most power system operators choose the larger value of the above two metrics, while others consider their aggregation. When there is a UHVDC injection in the power system, an equivalent largest unit is the UHVDC injection. Under such a scheme, the contingency reserve capacity will be no less than the UHVDC capacity. The extra cost associated with this scheme is increased operation cost of the entire power system:

$$C_1 = C_{\text{op}} - C_{\text{op}}^0. \tag{1}$$

2) Partial Load Shedding Scheme

An alternative scheme is to allocate the contingency reserve as a fraction of the UHVDC capacity and allow some imbalance during the contingency, which can be met by shedding load or employing demand response schemes. The advantages of such a scheme is that it reduces the reserve needed from conventional generation; however, it also experiences high economical losses from load shedding during a contingency. When there is a UHVDC injection in the power system, the associated extra cost includes both the operation cost and load shedding loss or demand response cost:

$$C_2 = C_{\text{op}} + C_{\text{ls}} - C_{\text{op}}^0. \tag{2}$$

3) Inter-area Sharing Scheme

The power system exchanges energy with neighboring systems through transmission interconnections. Contingency reserves for different power systems can also be shared through the transmission connection lines. Under the UHV DC and AC combined system, the UHVAC is able to make a strong connection between provincial power systems and also provide strong backups for contingency. This scheme requires the spare capacity of UHVAC transmission lines and transformers, which means that part of the UHVAC investment should be considered in the cost of this scheme:

$$C_3 = C_{\text{op}} + C_{\text{in}} - C_{\text{op}}^0 \tag{3}$$

B. Evaluation of Cost

1) Operation Cost

Operational costs include fixed cost, startup cost, and variable cost, all of which are determined by the dispatched output of generation.

The operation cost can be calculated using the probabilistic production simulation method or sequential operation simulation method. Since the probabilistic simulation method cannot reproduce generation dispatch, it also cannot accurately calculate startup and variable costs. Operation simulation, on the other hand, is essentially an annual hour by hour unit commitment approach, which is able to give an accurate operation mode of each unit and a more precise estimation to the operation cost of power system [15]. As such, the operation cost is calculated using the operation simulation method, which will be described in Section III in detail.

2) Load Shedding Cost

In this paper, the partial load shedding scheme only considers the UHVDC blocking fault. We use the classical expectation model to estimate the load shedding cost [23]. There are two kinds of UHVDC blocking faults: monopole trip and bipole trip. Both blocking faults contribute to the expected energy not served. Using the value of loss of load, the cost of loss of load can be calculated as follows.

$$C_{\text{ls}} = \mathit{VOLL} \times \mathit{EENS} \tag{4}$$

$$\mathit{EENS} = \mathit{EENS}_{\text{monopole}} + \mathit{EENS}_{\text{bipole}}. \tag{5}$$

With the assumption that the UHVDC transfers its rated power for 8760 hours, based on the fact that blocking faults do not occur, the normal energy transferred would be $8760P_{\text{DC}}$. Under these conditions, if there are no contingency reserves, then the energy loss caused by UHVDC the monopole and bipole blocking faults would be $8760p_{\text{el}}p_{\text{m}}P_{\text{DC}}$ and $8760p_{\text{el}}p_{\text{b}}P_{\text{DC}}$, respectively. Accordingly the power shortage would be $P_{\text{DC}}/2$ and P_{DC}, respectively. By accounting for the fact that the contingency reserve is able to compensate part of the power shortage, the energy loss would decrease to a ratio of $\frac{f(P_{\text{DC}}/2-R_{\text{con}})}{P_{\text{DC}}/2}$ and $\frac{f(P_{\text{DC}}-R_{\text{con}})}{P_{\text{DC}}}$. The *EENS* caused by the monopole and bipole blocking fault can be estimated as:

$$\mathit{EENS}_{\text{monopole}} = P_{\text{DC}} \cdot 8760 \cdot p_{\text{el}} \cdot p_{\text{m}} \frac{f(P_{\text{DC}}/2 - R_{\text{con}})}{P_{\text{DC}}/2} \tag{6}$$

$$\mathit{EENS}_{\text{bipole}} = P_{\text{DC}} \cdot 8760 \cdot p_{\text{el}} \cdot p_{\text{b}} \frac{f(P_{\text{DC}} - R_{\text{con}})}{P_{\text{DC}}}. \tag{7}$$

Function $f(\cdot)$ is given by

$$f(x) = \begin{cases} 0, & x \le 0 \\ x, & x > 0. \end{cases} \tag{8}$$

3) Investment Cost

To calculate the transmission line investment cost, the uniform annual value method is used to annualize the investment cost of the UHV line [24].

The investment cost C_i is accounted by the share of the total UHVAC investment, which is a specific fraction of the total capacity of UHVAC projects as follows:

$$C_{\text{in}} = \frac{P_{\text{DC}} - R_{\text{con}}}{N \cdot P_{\text{AC}}} \cdot (I_{\text{line, annual}} + I_{\text{trans, annual}}) \tag{9}$$

$$I_{\text{line, annual}} = I_{\text{line}} \cdot l \cdot \frac{i(1+i)^n}{(1+i)^n - 1} \tag{10}$$

$$I_{\text{trans, annual}} = I_{\text{trans}} \cdot m \cdot \frac{i(1+i)^n}{(1+i)^n - 1}. \tag{11}$$

III. Operation Simulation Model

Operation simulation is a type of long-term simulation method for power system planning based on daily unit commitment. Compared with probabilistic production method, operation simulation accurately estimates the operation cost while considering the operation requirements of the power system. In this paper, the operation simulation model in the GOPT software platform [15] is used to assess the operation cost of different contingency reserve allocation schemes.

A. Operation Simulation Process

As Fig. 1 shows, operation simulation consists of 4 steps.

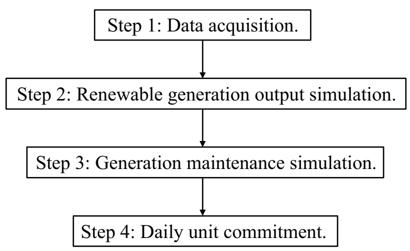

Fig. 1. Procedure of operation simulation.

Step 1: Data acquisition. The data needed for the operation simulation includes the load profile, parameters of units, and the boundary condition of interconnected lines. Round-the-year load profile of the target year's 8760 hours is required, which is usually generated using the historical load profile and the forecasted load level of the target year. Parameters of generating units such as output limit, ramp rate, and minimum start-up time are required to make the unit dispatches as realistic as possible. The inter-area energy transfer is also needed as boundary conditions of the simulation.

Step 2: Renewable generation output simulation. Chronological outputs of wind and solar power are simulated to reflect intermittency. The stochastic differential equation based simulation technique is proposed as in [16]–[18]. This method takes into consideration the probability distribution, spatial and temporal correlations, seasonal rhythms, and diurnal patterns of wind and solar power.

Step 3: Generation maintenance simulation. Generation maintenance determines the daily units that can be committed. A heuristic solution algorithm is used to arrive at an optimum plan with the objective of equal reserve rate among different days [19]. The model considers the need for continuity in the maintenance, exclusive constraints of units in the same plant, and available time constraint of units.

Step 4: Daily unit commitment. This is used to schedule the operation of all of the units with the objective of minimizing the overall generation cost of the power system. Unit commitment is conducted day-by-day throughout the target year. The state of each unit in the simulated day is considered as the boundary condition of the next day.

B. Daily Unit Commitment Model

The daily unit commitment model used in this paper can be seen fully in the Appendix. The objective function is to minimize the system operating cost, including fuel, start-stop, and load shedding costs, as well as wind curtailment costs.

The constraints mainly contain four aspects:

1) Load-Generation Balance Constraint: This constraint forces the sum of the power output of all the units equals to the load minus shedding load.

2) Generator Output Constraint: The power output of all generators is limited to their output interval.

3) Thermal Generation Ramp Rate Limit: This constraint limits the thermal generators' increasing or decreasing hourly power output to the ramp rate.

4) Maximum Daily Energy Production of Hydro and Pumped Storage Units: Reservoir capacity limits put constraints of maximum daily energy production on hydro and pumped storage units.

To simplify the issues, the power grid topology constraint is neglected. In order to highlight the key constraint considered in this paper, the reserve constraint is changed, as the next section states.

C. Modeling of Contingency Reserve

The contingency reserve, as well as the regulative reserve is modeled as a constraint in the operation simulation model (A9). Constraint (A9) guarantees that the capacity of the online generator meets the demand of regulating and the contingency reserve requirements.

In operation simulation, UHVAC is modeled as a special type of unit, whose output is assigned as fixed curves according to the inter-area delivery contract.

The model forms a standard Mixed Integer Linear Programming (MILP) model. All of the steps of the operation simulation are implemented using the C programming language. The unit commitment model is solved using CPLEX optimization pack.

IV. Case Study

A techno-economic evaluation of the contingency reserve scheme of Jiangsu power system is carried out. This study is based on a planning scheme for the year 2018, at which time the Jiangsu power system is expected to be finally connected to other provinces via the UHVDC or UHVAC transmission lines. Fig. 2 shows the interconnections of Jiangsu province according to the planning of the State Grid Corporation. Jiangsu province will be connected with Shandong, Anhui, Shanghai by three double-circuit 1000 kV UHVAC lines. The electricity from the pithead power plants in Inner Mongolia and Shanxi province will be delivered to Jiangsu province through the Ximeng ± 800 kV UHVDC and the Jinbei ± 800 kV UHVDC lines, respectively.

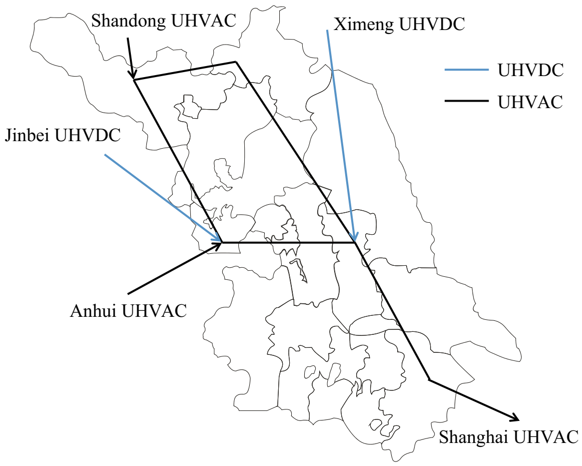

Fig. 2. Jiangsu UHV DC and AC combined system.

The calculation was conducted using a Windows-based PC with four threads clocking at 2.5 GHz and 8 GB RAM. It takes 32 minutes to simulate the annual 2018 operations of the Jiangsu system.

The case study consists of five parts: 1) basic parameters, 2) case settings, 3) operation simulation analysis, 4) cost results, and 5) sensitivity analysis. The first two parts provide an analysis of the power system with different reserve allocation schemes. The third part carries out the detailed simulation results of the target power system, showing how it is operated under different reserve allocation schemes. The fourth part presents the cost associated with each reserve allocation scheme. Finally, a sensitivity analysis is conducted to demonstrate the robustness of our result.

A. Basic Parameters of Jiangsu Power System in 2018

1) Load Forecast

According to the planning scheme, the peak load of Jiangsu will reach 106 GW during afternoons in summer, when air conditioner loads are very high. The minimum load appears at midnight during winter, which is only 28 GW, as seen in Fig. 3. The entire year's electricity consumption will reach 618 TWh from 501 TWh in 2014. The hourly variation of load in 2018 is assumed to follow the same patterns as in 2014 [20]. So the load profile of 2018 can be arrived at based on the rule of proportion.

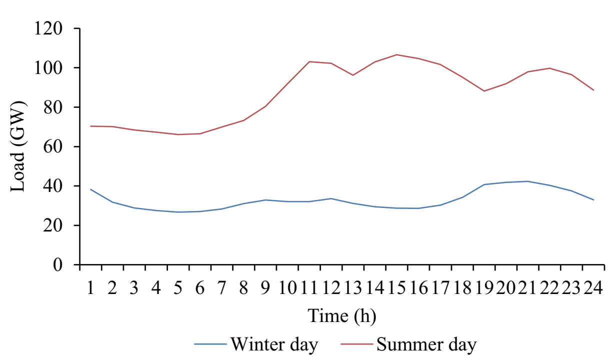

Fig. 3. Forecasted load of the maximum load and minimum load day of Jiangsu Province.

2) Generation Planning

The generation capacity of the Jiangsu power system in 2018 will reach 141 GW, when taking the inter-area connection into account. The generation portfolio is shown in Fig. 4. The Jiangsu power system is divided into eight units: 1) nuclear, 2) large coal fired, 3) small coal fired, 4) gas fired, 5) pumped storage, 6) wind, 7) UHVAC, and 8) UHVDC. Coal fired units take the major share (about 51%) of Jiangsu power system. Large coal fired units contribute to the base load and part of the shoulder load. There are 3% of nuclear units that usually maintain a constant output, contributing to the base load. The Jiangsu power system has 14% small coal fired units and 12% gas fired units, as well as 2% pumped storage units for peak load regulation. The capacity of wind power takes 7% of the total generation. The capacity of UHVDC and UHVAC units take the share of 17% and 8%, respectively.

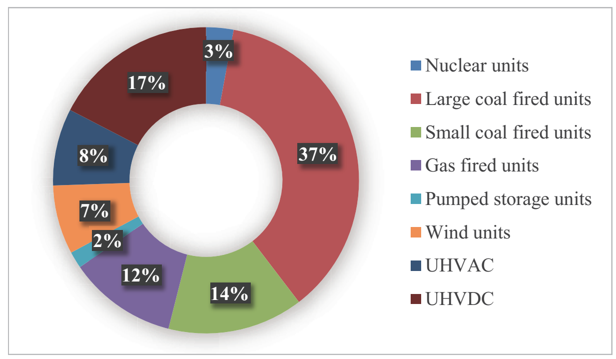

Fig. 4. Generation portfolio of Jiangsu power system.

3) UHVDC Projects

The designed capacity of Ximeng and Jinbei UHVDC are 10 GW and 8 GW, respectively. Therefore, the blocking fault of Ximeng UHVDC is chosen as the reference of contingency reserves. Its reliability parameters, shown in Table I, are extracted from the country's average statistics of current operating UHVDC projects [21].

TABLE I
XIMENG UHVDC RELIABILITY PARAMETERS

Parameters	Value
Capacity (GW)	10
Forced energy loss rate (%)	1.00
Bipole outage times (times/year)	0.25
Monopole outage times (times/year)	2.6
Bipolar outage energy percentage (%)	16.13
Unipolar outage energy percentage (%)	83.87

4) North-Central-East China UHVAC Parameters

The investment cost and rated capacity of the Jiangsu power planning scheme are shown in Table II [22]. The length and the spared contingency reserve capacity of the UHVAC lines linking Jiangsu with Shandong, Anhui, and Shanghai are set in Table III.

5) Cost of Load Shedding

Since currently there is no reference for VOLL in Jiangsu province, the Texas VOLL value as in [23] is assumed to be

TABLE II
UHVAC INVESTMENT COST PARAMETERS

Parameters	Value
Investment cost of lines (million Yuan/km)	15.0
Rated capacity (GW)	6.0
Investment cost of transformer (billion Yuan)	1.0
Number of transformers	6

TABLE III
UHVAC INVESTMENT COST PARAMETERS

Connection	Length (km)	Contingency Reserve Capacity (GW)
Shandong	67.4	2.27
Anhui	150	2.27
Shanghai	83	2.27

equal to that of Jiangsu province. The exchange rate of RMB Yuan to USD is assumed to be 6.35, as shown in Table IV.

TABLE IV
LOAD SHEDDING ECONOMIC DATA

Items	Value
VOLL (US$/MWh)	6,000
Exchange rate (¥/$)	6.35

B. Case Settings

1) Traditional Scheme

Since the fault of Ximeng HVDC is the largest single fault in Jiangsu province, in this scheme the contingency reserve equals to the capacity of Ximeng HVDC (10 GW).

2) Partial Load Shedding Scheme

The second scheme sets the contingency reserve to be a fraction of the capacity of Ximeng HVDC. Three sub schemes are designed with contingency reserves of 8 GW, 6 GW, and 4 GW.

3) Inter-Area Sharing Scheme

The third scheme takes the traditional contingency reserve allocation method, which makes the contingency reserve equal to 3% of the load at 3.18 GW. It is also assumed that the UHVAC will provide enough support during the UHVDC blocking fault.

C. Operation Simulation Analysis

The year-round operation of Jiangsu power system under each of the schemes is simulated using GOPT. Fig. 5 illustrates the scheduling of units on a typical day under the traditional scheme. Results show that the UHVAC and UHVDC mainly hold the base load, and the coal fired units balance both the base and shoulder loads. The gas fired units and pumped storage units serve the peak load.

The equivalent full generation hours of different type of units under different schemes are shown in Fig. 6. The result shows that equivalent full generation hours among different schemes are essentially the same, suggesting that the variable cost among different schemes would be similar. A closer comparison shows that generation hours of small coal fired units has a slight drop and that of pumped storage has a small increase as the contingency reserve requirement reduces from 10 GW to 3.18 GW (3% of the load). The result reveals that

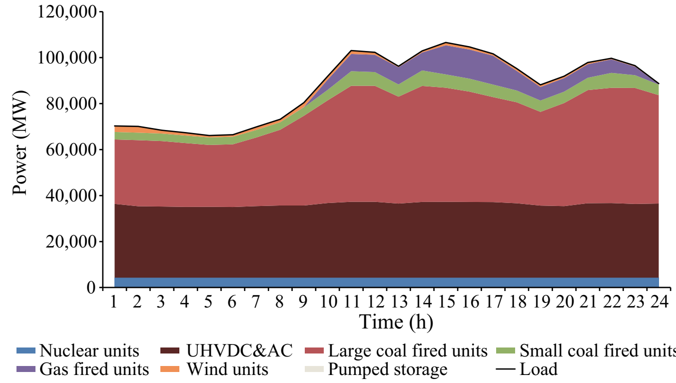

Fig. 5. Scheduling of different kind of units on a typical summer day under the traditional scheme.

higher contingency reserve requirement would force the small coal fired units to be scheduled to enhance the reserve, and the pumped storage is utilized to compensate for the inflexibility of the small coal fired units.

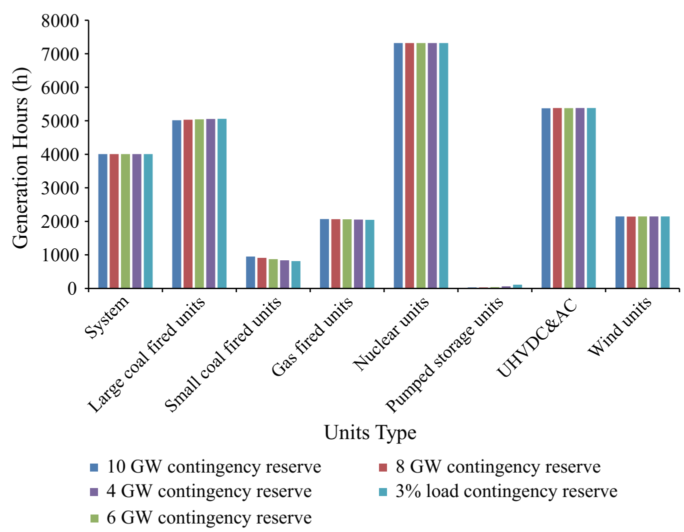

Fig. 6. Equivalent full generation hours of different units in different schemes.

Fig. 7 shows the hourly maximum and minimum output of units committed in different contingency reserve schemes. The result shows that more units are committed as the contingency reserve requirements increase, suggesting that more fixed operating costs will occur. However, we can also see that the maximum output of units committed to under 8 GW and 6 GW are very close, which means that the fixed cost of the two schemes are close to each other. Fig. 6 shows that the generation hours are close, suggesting that the variable cost would also be close. Thus the main difference of total cost would be caused by load shedding cost.

D. Cost Results

Table V lists the breakdown of the costs associated with three contingency reserve allocation schemes. The extra cost of the traditional scheme which takes 10 GW contingency reserve is 2.66 billion Yuan. The partial load shedding schemes have a much higher cost of 3.29 billion Yuan, 3.80 billion Yuan, 7.20 billion Yuan for 8 GW, 6 GW, and 4 GW contingency reserve,

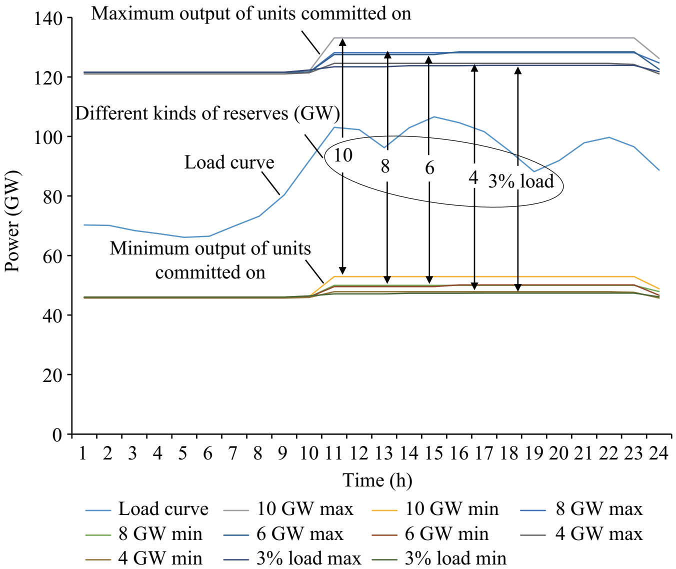

Fig. 7. Hourly maximum and minimum output of unit committed in different contingency reserve schemes.

respectively. The inter-area sharing scheme has the least extra cost, which is 0.37 billion Yuan.

TABLE V
COST OF THREE CONTINGENCY RESERVE ALLOCATION SCHEMES (IN BILLION YUAN)

Items	Traditional Scheme	Partial Load Shedding Scheme			Interarea Sharing Scheme
Contingency reserve (GW)	10	8	6	4	3% load
Variable cost	153.04	152.76	152.49	152.30	152.15
Startup cost	0.71	0.63	0.55	0.45	0.39
Fixed cost	17.52	17.42	17.21	16.38	16.06
Operation cost	171.26	170.81	170.25	169.13	168.60
Load shedding cost	0.00	1.08	2.15	6.68	0.00
Investment cost	0.00	0.00	0.00	0.00	0.37
Total cost	171.26	171.89	172.40	175.80	168.97
Extra cost	2.66	3.29	3.80	7.20	0.37

Fig. 8 compares the costs among different contingency reserve schemes. The operation cost, represented by the yellow line, decreases as the contingency reserve reduces. However, the operation costs are very close among different schemes just as we have analyzed above. The changes mainly come from the fixed operation cost, which reflects the fact that the contingency reserves require more generators to be committed. The variable cost also decreases a little with less contingency reserves since the load factor of generators are higher.

The results show that extra cost of contingency reserve differs enormously among the three types of schemes. The reasons are three folds:

1) The VOLL is much higher compared with the generation cost.
2) The quantity of energy not served is large when the UHVDC blocks.
3) The investment associated with the transmission capacity of UHVAC is much lower compared with the cost of load shedding.

Thus the economic loss from energy loss of the UHVDC blocking fault would be so large that it should be compensated for by more reserve allocation. The investment of the UHVAC line of the inter-area sharing scheme is small when compared with the operation cost of more reserve in the single area; the most cost efficient choice would be therefore the inter-area sharing scheme.

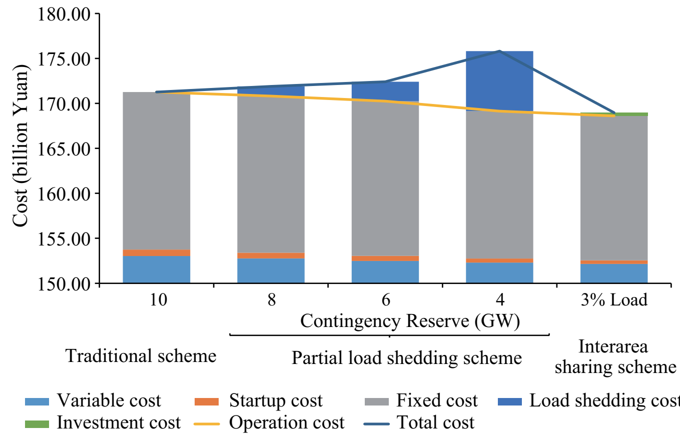

Fig. 8. Comparison of the cost between different contingency reserve allocation schemes.

E. Sensitivity Analysis

Since load shedding cost is driven by VOLL and the annualized investment of UHVAC system depends on the discount rate, a sensitivity analysis is carried out to quantify the robustness of our conclusion.

Fig. 9 shows the impact of VOLL on the difference of cost between the traditional scheme and the first partial load shedding scheme. The cost difference decreases linearly from 0.625 to 0.286 billion Yuan/year as VOLL decreases from 38,000 to 26,000 Yuan/MWh. The breakeven point of VOLL is 15,860 Yuan/MWh, which means that the traditional scheme is always better than the partial load shedding scheme when the VOLL is higher than 15,860 Yuan/MWh. The result means that if the VOLL is in a reasonable range, the traditional scheme would always be more cost-efficient than the partial load shedding scheme.

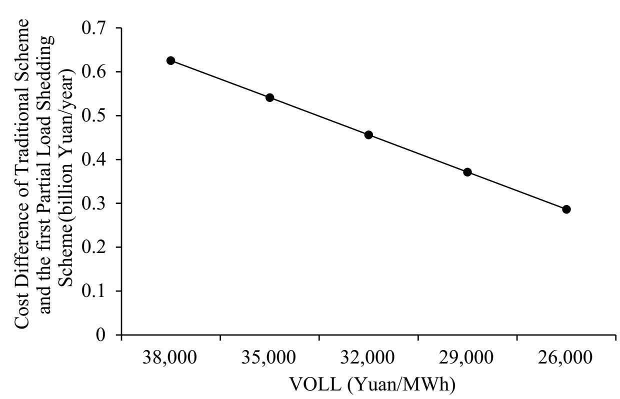

Fig. 9. Effect of VOLL to the cost difference between the traditional scheme and the first partial load shedding scheme.

Fig. 10 shows the impact of discount rate on the difference of cost between the traditional scheme and the inter-area sharing scheme. The cost difference decreases from 2.28 to 2.00 billion Yuan/year as the discount rate increases from 0.08 to 0.16. The break-even point of discount rate is 0.67, which means that the inter-area sharing scheme is always better than the traditional scheme when the discount rate is lower than 0.67. This result also means that the inter-area sharing scheme would always be more cost-efficient than the traditional scheme, irrespective of small variations of discount rate being within a large range.

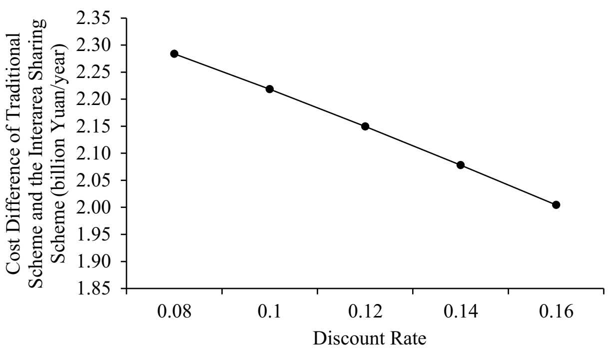

Fig. 10. Effect of discount rate to the cost difference between traditional scheme and the inter-area sharing scheme.

Overall, the inter-area sharing scheme is always the best reserve allocation scheme when the change of VOLL and discount rate are taken into account.

V. Conclusion

This paper analyzes the contingency reserve allocation schemes of the receiving end of the UHV DC and AC combined system. An operation simulation based method is proposed to evaluate the costs of providing extra contingency reserves for HVDC blocking fault. Three contingency reserve schemes are designed and analyzed for the Jiangsu provincial power system in China. The results show that sharing the contingency reserve with a neighboring power system thorough UHVAC transmission lines is the most cost-efficient scheme for the Jiangsu power system in 2018. A sensitivity analysis of VOLL and discount rate proves that our result is robust with the variation of parameters.

Appendix

A. Mathematical Model

The full unit commitment model used in this paper is as follows.

1) Object Function

The objective is the minimization of the total system operation cost, which includes the fuel, start-stop, load shedding cost as well as the penalty for wind and solar curtailment.

$$\min C_{\text{sys}} = \sum_{t\in\Omega} \begin{aligned}&(\boldsymbol{C}_{\text{f}}^{\text{T}}\boldsymbol{P}_{\text{f}}^{t} + \boldsymbol{C}_{\text{c}}^{\text{T}}\boldsymbol{P}_{\text{c}}^{t} + \boldsymbol{C}_{\text{w}}^{\text{T}}\boldsymbol{P}_{\text{w}}^{t} + \boldsymbol{C}_{\text{s}}^{\text{T}}\boldsymbol{P}_{\text{s}}^{t} + \\ &\eta\boldsymbol{C}_{\text{wd}}^{\text{T}}\boldsymbol{P}_{\text{wd}}^{t} + \delta\boldsymbol{C}_{\text{sd}}^{\text{T}}\boldsymbol{P}_{\text{sd}}^{t} + \theta\boldsymbol{C}_{\text{d}}^{\text{T}}\boldsymbol{D}_{\text{d}}^{t} + \gamma[1]^{\text{T}}\boldsymbol{S}_{\text{f}}^{t})\end{aligned} \tag{A1}$$

2) Constraints

The constraints include load generation balance constraint, output interval constraint, positive and negative reserve constraint, generation ramp rate constraint, hydro and pumped storage energy constraint.

$$\begin{aligned}&[1]^{\text{T}}\boldsymbol{P}_{\text{f}}^{t} + [1]^{\text{T}}\boldsymbol{P}_{\text{c}}^{t} + [1]^{\text{T}}\boldsymbol{P}_{\text{w}}^{t} + [1]^{\text{T}}\boldsymbol{P}_{\text{h}}^{t} - [1]^{\text{T}}\boldsymbol{D}_{\text{h}}^{t} + [1]^{\text{T}}\boldsymbol{D}_{\text{d}}^{t} \\ &= [1]^{\text{T}}\boldsymbol{D}^{t}, \forall t\in\Omega\end{aligned} \tag{A2}$$

$$\boldsymbol{P}_{\text{f}\min}\boldsymbol{I}_{\text{f}}^{t} \le \boldsymbol{P}_{\text{f}}^{t} \le \boldsymbol{P}_{\text{f}\max}\boldsymbol{I}_{\text{f}}^{t}, \forall t\in\Omega \tag{A3}$$

$$\boldsymbol{P}_{\text{c}\min}\boldsymbol{I}_{\text{c}} \le \boldsymbol{P}_{\text{c}}^{t} \le \boldsymbol{P}_{\text{c}\max}\boldsymbol{I}_{\text{c}}, \forall t\in\Omega \tag{A4}$$

$$\max[\boldsymbol{P}_{\text{h}\min}, \boldsymbol{0}] \le \boldsymbol{P}_{h}^{t} \le \boldsymbol{P}_{h\max}, \forall t\in\Omega \tag{A5}$$

$$\boldsymbol{0} \le \boldsymbol{D}_{\text{h}}^{t} \le -\boldsymbol{P}_{\text{h}\min}, \forall t\in\Omega \tag{A6}$$

$$\boldsymbol{P}_{\text{w}}^{t} + \boldsymbol{P}_{\text{wd}}^{t} = \boldsymbol{P}_{\text{wf}}^{t}, \boldsymbol{0} \le \boldsymbol{P}_{\text{w}}^{t}, \boldsymbol{0} \le \boldsymbol{P}_{\text{wd}}^{t}, \forall t\in\Omega \tag{A7}$$

$$\boldsymbol{S}_{\text{f}}^{t} \ge \boldsymbol{V}_{\text{f}} * (\boldsymbol{I}_{\text{f}}^{t} - \boldsymbol{I}_{\text{f}}^{t-1}), \boldsymbol{S}_{\text{f}}^{t} \ge \boldsymbol{0}, \forall t\in\Omega \tag{A8}$$

$$\begin{aligned}&(1 + r_{\text{reg}})[1]^{\text{T}}\boldsymbol{D}_{t} + R_{\text{con}} \le [1]^{\text{T}}\boldsymbol{P}_{\text{f}\max}\boldsymbol{I}_{\text{f}}^{t} + [1]^{\text{T}}\boldsymbol{P}_{\text{c}\max}\boldsymbol{I}_{\text{c}} \\ &+ [1]^{\text{T}}\boldsymbol{P}_{\text{wf}}^{t} + [1]^{\text{T}}\boldsymbol{P}_{\text{sf}}^{t} + [1]^{\text{T}}\boldsymbol{P}_{\text{h}\max} + [1]^{\text{T}}\boldsymbol{D}_{\text{d}}^{t}, \forall t\in\Omega\end{aligned} \tag{A9}$$

$$\begin{aligned}&(1 - r_{\text{reg}})[1]^{\text{T}}\boldsymbol{D}_{t} \ge [1]^{\text{T}}\boldsymbol{P}_{\text{f}\min}\boldsymbol{I}_{\text{f}}^{t} + [1]^{\text{T}}\boldsymbol{P}_{\text{c}\min}\boldsymbol{I}_{\text{c}} \\ &+ [1]^{\text{T}}\min[\boldsymbol{P}_{\text{h}\min}, 0] + [1]^{\text{T}}\boldsymbol{D}_{\text{d}}^{t}, \forall t\in\Omega\end{aligned} \tag{A10}$$

$$\begin{aligned}&-\Delta\boldsymbol{P}_{\text{fdown}} \le \boldsymbol{P}_{\text{f}}^{t} - \boldsymbol{P}_{\text{f}}^{t-1} \le \Delta\boldsymbol{P}_{\text{fup}} \\ &-\Delta\boldsymbol{P}_{\text{cdown}} \le \boldsymbol{P}_{\text{c}}^{t} - \boldsymbol{P}_{\text{c}}^{t-1} \le \Delta\boldsymbol{P}_{\text{cup}}, \forall t\in\Omega\end{aligned} \tag{A11}$$

$$\sum_{t\in\Omega}\boldsymbol{P}_{\text{h}}^{t} \le \boldsymbol{G}_{\text{h}} \tag{A12}$$

$$\boldsymbol{\lambda}^{\text{T}}\sum_{t\in\Omega}\boldsymbol{D}_{\text{h}}^{t} = \sum_{t\in\Omega}\boldsymbol{P}_{\text{h}}^{t}, \forall\boldsymbol{P}_{\text{h}\min} \le \boldsymbol{0} \tag{A13}$$

$$\boldsymbol{I}_{\text{f}}^{t} \in \{0,1\}, \forall t\in\Omega, \boldsymbol{I}_{\text{c}} \in \{0,1\} \tag{A14}$$

$$\boldsymbol{D}_{\text{d}}^{t} \ge \boldsymbol{0}, \forall t\in\Omega \tag{A15}$$

B. Operation Cost

The fixed cost, variable cost and startup cost are calculated as Table AI which comes from the report [20].

TABLE AI
Operation Cost of Different Kinds Of Units

Generation Type	Capacity (MW)	Fixed Cost (Yuan/kW)	Minimum Output (MW)	Variable Cost (Yuan/MWh)		Startup Cost (Yuan)
				Max Output	Min Output	
Thermal generation	135	96	54	31.6	33.1	102,552
	200	96	80	30.1	31.5	205,105
	300	96	150	28.6	30.1	307,638
	330	78	165	28.0	29.4	338,404
	600	78	360	27.0	28.3	615,283
	1,000	68	600	25.8	27.1	1,025,468
NGCC	180	81	90	59.4	62.5	0
PHS	300	56	−300	0.0	0.0	0
Hydro	100–180	184	0	0.0	0.0	0
Wind power	1.5–3.0	103	0	0.0	0.0	0

References

[1] D. C. Huang, Y. B. Shu, J. J. Ruan, and Y. Hu, “Ultra high voltage transmission in China: Developments, current status and future prospects,” *Proceedings of the IEEE*, vol. 97, no. 3, pp. 555–583, Mar. 2009.

[2] A. J. Wood, B. F. Wollenberg and G. B. Sheble, *Power Generation, Operation, and Control,* 3rd ed., vol. I. New York: Wiley, 2013, p. 150.

[3] Z. Xu, H. F. Dong, and H. Y. Huang, “Debates on ultra-high-voltage synchronous power grid: the future super grid in China?” *IET Generation, Transmission & Distribution*, vol. 9, no. 8, pp. 740–747, May 2015.

[4] D. R. Bobo, D. M. Mauzy, and F. J. Trefny, “Economic generation dispatch with responsive spinning reserve constraints,” *IEEE Transactions*

on Power Systems, vol. 9, no. 1, pp. 555–559, Feb. 1994.

[5] R. Billinton, L. Salvaderi, J. D. McCalley, H. Chao, T. Seitz, R. N. Allan, J. Odom, and C. Fallon, "Reliability issues in today's electric power utility environment," *IEEE Transactions on Power Systems*, vol. 12, no. 4, pp. 1708–1714, Nov. 1997.

[6] R. Doherty and M. O. Malley, "A new approach to quantify reserve demand in systems with significant installed wind capacity," *IEEE Transactions on Power Systems*, vol. 20, no. 2, pp. 587–595, May 2005.

[7] H. B. Gooi, D. P. Mendes, K. R. W. Bell, and D. S. Kirschen, "Optimal scheduling of spinning reserve," *IEEE Transactions on Power Systems*, vol. 14, no. 4, pp. 1485–1492, Nov. 1999.

[8] F. Bouffard, F. D. Galiana, and A. J. Conejo, "Market-clearing with stochastic security, Part I: Formulation," *IEEE Transactions on Power Systems*, vol. 20, no. 4, pp. 1818–1826, Nov. 2005.

[9] S. Wong and J. D. Fuller, "Pricing energy and reserves using stochastic optimization in an alternative electricity market," *IEEE Transactions on Power Systems*, vol. 22, no. 2, pp. 631–638, May 2007.

[10] A. Street, A. Moreira, and J. M. Arroyo, "Energy and reserve scheduling under a joint generation and transmission security criterion: An adjustable robust optimization approach," *IEEE Transactions on Power Systems*, vol. 29, no. 1, pp. 3–14, Jan. 2014.

[11] Y. Ding, M. Xie, Q. W. Wu, and J. Stergaard, "Development of energy and reserve pre-dispatch and re-dispatch models for real-time price risk and reliability assessment," *IET Generation, Transmission & Distribution,* vol. 8, no. 7, pp. 1338–1345, Jul. 2014.

[12] Z. Zhou and A. Botterud, "Dynamic scheduling of operating reserves in co-optimized electricity markets with wind power," *IEEE Transactions on Power Systems*, vol. 29, no. 1, pp. 160–171, Jan. 2014.

[13] J. D. Lyon, F. Y. Wang, K. W. Hedman, and M. H. Zhang, "Market implications and pricing of dynamic reserve policies for systems with renewables," *IEEE Transactions on Power Systems,* vol. 30, no. 3, pp. 1593–1602, May 2015.

[14] Y. Wang, B. Liu, T. B. Liu, and H. S. Sun, "Coordinated optimal dispatching of emergency power support among provinces after UHVDC transmission system block fault," *Proceedings of the CSEE*, vol. 35, no. 11, pp. 2695–2702, Jun. 2015 (in Chinese).

[15] N. Zhang, C. Q. Kang, D. S. Kirschen, Q. Xia, W. M. Xi, J. H. Huang, and Q. Zhang, "Planning pumped storage capacity for wind power integration," *IEEE Transactions on Sustainable Energy*, vol. 4, no. 2, pp. 393–401, Apr. 2013.

[16] N. Zhang, C. Q. Kang, C. G. Duan, X. J. Tang, J. J. Huang, Z. Lu, W. Z. Wang, and J. Q. Qi, "Simulation methodology of multiple wind farms operation considering wind speed correlation," *International Journal of Electrical Power & Energy Systems*, vol. 30, no. 4, pp. 264–273, Dec. 2010.

[17] X. Zhang, C. Q. Kang, N. Zhang, Y. H. Huang, C. Liu, and J. F. Xu, "Analysis of mid/long term random characteristics of photovoltaic power generation," *Automation of Electric Power Systems*, vol. 38, no. 6, pp. 6–13, Mar. 2014 (in Chinese).

[18] W. J. Zhao, N. Zhang, C. Q. Kang, Y. F. Wang, P. Li, and S. Ma, "A method of probabilistic distribution estimation of conditional forecast error for photovoltaic power generation," *Automation of Electric Power Systems*, vol. 39, no. 16, pp. 8–15, Aug. 2015 (in Chinese).

[19] U. Basaran and M. Kurban, "The strategy for the maintenance scheduling of the generation units," in *Proceedings of 2003 Large Engineering Systems Conference on Power Engineering (LESCOPE)*, May 2003, pp. 172–176.

[20] N. Zhang, X. Lu, M. B. McElroy, C. P. Nielsen, X. Y. Chen, Y. Deng, and C. Q. Kang, "Reducing curtailment of wind electricity in China by employing electric boilers for heat and pumped hydro for energy storage," *Applied Energy*, Dec. 2015, DOI: 10.1016/j. apenergy.2015.10.147.

[21] X. Q. Yu, "Statistics and analysis on reliability of HVDC power transmission systems of State Grid Corporation of China," *Power System Technology*, vol. 33, no. 12, pp. 1–7, Jun. 2009 (in Chinese).

[22] "Power generation planning optimization of Jiangsu province," Jiangsu Electric Power Company, Nanjing, China, May 2010 (in Chinese).

[23] B. Magness and C. V. Seely. (2013, Jun.). Estimating the value of lost load: Briefing paper prepared for ERCOT by LEI. London Economics International LLC, Boston, MA. [Online]. Available: https://www.hks.harvard.edu/hepg/Papers/2013/06%2018%2013%20ERCOT%20VOLL%20Literature%20Review%20and%20Macroeconomic%20Analysis_0613.pdf

[24] R. Romero, A. Monticelli, A. Garcia, and S. Haffner, "Test systems and mathematical models for transmission network expansion planning," *IEE Proceedings – Generation, Transmission and Distribution*, vol. 149, no. 1, pp. 27–36, Jan. 2002.

Di Wu (S'14) received the B.S. degree from the Department of Electrical Engineering in Tsinghua University, Beijing, China, in 2014. He is currently pursuing Ph.D. degree in Tsinghua University. His research interests include power system planning, operation and the control of carbon capture and sequestration plants.

Ning Zhang (M'12) received the B.S. and Ph.D. degree from the Department of Electrical Engineering, Tsinghua University, Beijing, China, in 2007 and 2012, respectively. He is currently a Lecturer at the same university. His research interests include power system planning with renewable energy, renewable energy statistic characteristic analysis and operation simulation, and power system dispatching with renewable energy.

Chongqing Kang (M'01–SM'08) received the Ph.D. degree from the Department of Electrical Engineering in Tsinghua University, Beijing, China, in 1997. He is currently a Professor at the same university. His research interests include load forecasting, electricity market, power system planning and generation scheduling optimization.

Yi Ge received the Ph.D. degree from the Department of Electrical Engineering, Queen's University, Belfast, North Ireland, in 2013. He is currently a staff member of Power System Planning Research Center, Economic Research Institute of Jiangsu Electric Power Company.

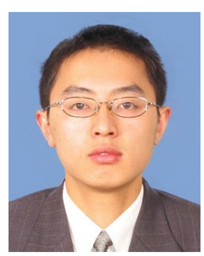

Zhenjian Xie received the B.S. degree from the Department of Electrical Engineering, Shanghai Jiao Tong University, Shanghai, China, in 2002. He is currently the Vice Director of Power System Planning Research Center, Economic Research Institute of Jiangsu Electric Power Company. He is now engaged in power system planning in Jiangsu province.

Junhui Huang received the B.S. degree from the Department of Electrical Engineering, Southeast University, Nanjing, China, in 1987. He is currently the Director of Power System Planning Research Center, Economic Research Institute of Jiangsu Electric Power Company.